WELDING RESEARCH

SUPPLEMENT TO THE WELDING JOURNAL, JULY 1986

Sponsored by the American Welding Society and the Welding Research Council

Readers are advised that all papers published in the *Welding Journal's* Research Supplement undergo Peer Review before publication for: 1) originality of the contribution; 2) technical value to the welding community; 3) prior publication of the material being reviewed; 4) proper credit to others working in the same area; and 5) justification of the conclusions based on the results.

The names of the more than 160 individuals serving on the AWS Peer Review Panel are published periodically. All are experts in their respective technical areas, and all are volunteers in the program.

Modelling the Fluid Flow in Laser Beam Welding

Interrelationships of absorbed laser beam power, weld width, speed, and keyhole size are evaluated

BY M. DAVIS, P. KAPADIA AND J. DOWDEN

ABSTRACT. The use of lasers in the welding of metals is becoming increasingly important in high technology industries. Accordingly, after a brief review of the literature, analytical and numerical results of two-dimensional models of the flow of the molten metal around the keyhole are discussed. This work illustrates the connection between the absorbed laser beam power, the weld width, the weld speed and the size of the keyhole for different metals. In conclusion, some interesting insight is gained into fluid dynamical flows of molten metal in the process of laser beam welding.

Introduction

This article considers fluid dynamical models of laser beam welding of metals using a continuous laser source as opposed to pulsed laser systems. The laser beam is usually directed almost perpendicularly to the workpiece, as shown in Fig. 1. Figure 2 is a photograph of a demonstration weld in progress on a circular pipe.

Initially, the beam creates a hole, but subsequently, as the workpiece is moved relative to the laser beam, this "keyhole" moves through the metal with only a small amount of matter lost by further vaporization. This keyhole is normally created in milliseconds by a well focussed high-intensity laser beam, usually that of a CW CO_2 laser. The light emitted from the CO_2 laser is in the infrared at a wavelength of 10.6 μm. This light output, as with all laser radiation, has a number of

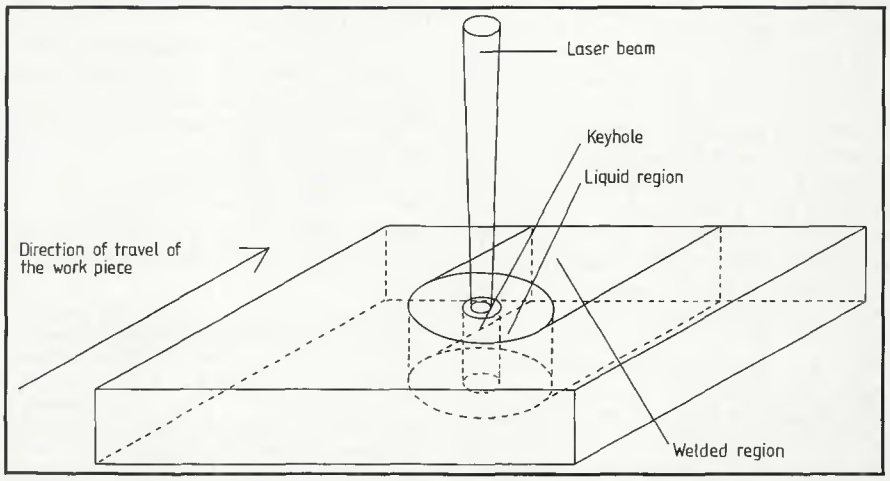

Fig. 1 — Geometry of the laser beam relative to the workpiece

M. DAVIS and P. KAPADIA are with the Department of Physics and J. DOWDEN is with the Department of Mathematics, University of Essex, Colchester, England.

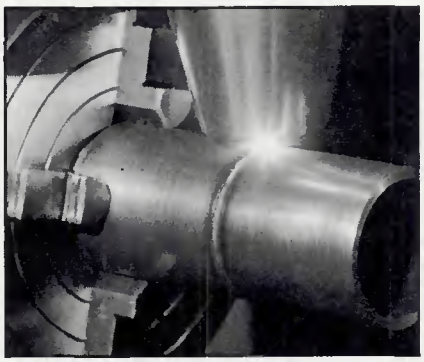

Fig. 2—Demonstration weld in progress on a circular pipe

unique properties: high intensity of electromagnetic energy flux, high monochromaticity and high spatial and temporal coherence. Hence, the beam can be focussed into a small spot (ranging in size from micrometers to a fraction of a millimeter), and this is of great importance in forming a good keyhole for deep-penetration welding. Coupling of the laser energy to the workpiece is achieved by direct irradiation, as well as through the formation of a plasma in the keyhole. This plasma is formed when the workpiece material evaporates and subsequently ionizes in the keyhole. The plasma absorbs energy from the incident laser beam predominantly by inverse Bremsstrahlung absorption by electrons in the field of ions and neutral atoms in the keyhole, and this energy is transferred to the metal as heat, mainly by conduction processes. Inadequate transfer of energy from the laser beam to the plasma, *i.e.*, if the laser intensity is too low, would cause its collapse. On the other hand, if the beam were too powerful, it causes "pluming," the excess production of plasma, which back reflects the laser light. Both of these conditions can lead to the possible collapse of the keyhole. So, for a continuous weld, a stable plasma regime is required. The keyhole can be regarded as an effective heat pipe and this results in the high efficiency of laser beam welding. It is probable that the keyhole is kept open by a combination of the pressure of the plasma that forms in the keyhole and the recoil pressure of the evaporating metal. The total pressure is in excess of atmospheric, and it will have two separate effects. One is to force the liquid metal outward so that it forms a weld bead on the surface of the completed weld. The other effect of the excess pressure in the keyhole is to force metal vapor out at either end. Since this would damage the optics of the laser, it is usual to provide a jet of helium or argon directed coaxially parallel to the laser beam as a shielding gas. The nozzle through which this gas flows is visible in Fig. 2. Argon (but not helium) ionizes and contributes to the plasma in the keyhole.

The energy supplied by the laser beam leads to melting of a region about the keyhole, whose cross-section is observed to be very close to circular. Metal then flows in this liquid region from the front of the hole to the rear, where it ultimately solidifies again, forming surface beads which normally enhance the mechanical properties of the weld.

Metallurgically, a weld made by a laser beam has relatively few impurities. As a result, the mechanical properties such as hardness, tensile strength and impact strength are the same as those of the base material and in some instances better. A full comparison, however, depends on a knowledge of the exact composition and prior heat treatment.

Laser beam welding offers many practical advantages: no welding filler rods, fluxes or protective materials are needed, while internal stresses and cracks are minimized. The flexibility of the laser beam and ease of handling, positioning and controlling lends itself to automatic operations as well as real-time computer control. Electron beam welding, which makes use of a focussed beam of electrons and has to be carried out in a vacuum, is now being replaced by laser beam welding, which does not.* Laser beam welding is also superior to conventional welding because it makes a weld with less overall heat input, with the result that the heat-affected area is a small one.

Review of the Literature

An extensive body of literature of mathematical analysis already exists on two aspects of the theory of welding, and a brief survey of the ideas involved has been given by Andrews (Ref. 1). The first of these uses fluid motion techniques involving high electric currents as employed in arc welding, while the second uses thermal analysis in which fluid motion is ignored.

Among the many treatments of the problem based on heat conduction methods, two typical papers are those of Mazumder and Steen (Ref. 2) and Swift-Hook and Gick (Ref. 3).

To avoid a detailed treatment of the keyhole, Mazumder and Steen used the device, for numerical calculation, in which points in the keyhole are treated as part of the metal but at a fictitiously high temperature, energy being conveyed to the metal by conduction.

Using a moving line source model, Swift-Hook and Gick attempted to show how the width and depth of the melted zone depends on laser power and the speed of translation of the workpiece. They solved the steady state heat diffusion equation in a moving medium. In particular, they discuss two limiting cases, referring to high and low speeds involving a relationship between the absorbed power and the weld width. They do not, however, treat the motion of the molten pool.

On the other hand, Andrews and Atthey (Ref. 4) used a hydrodynamic model to calculate the penetration depth, assuming a keyhole is drilled in a molten pool. They considered a steady state irrotational flow, including both the effects of surface tension and gravity in the formation of the keyhole.

In this article, we focus attention on the flow around the keyhole, as this is important in the formation of the weld.

The Modelling

In considering the modelling of the steady continuous laser beam welding process, the metal translates with a constant velocity U relative to a perpendicularly directed laser beam, and a description of the flow of metal around the keyhole as well as its temperature is sought.

For the purposes of obtaining analytical forms for the solution, two basic assumptions are made, that the motion is steady two-dimensional flow and that the Péclet number of the flow is small. In the model, the inner surface of the keyhole must be at or very close to the boiling point of the metal T_v, making this surface an isotherm. The heat transfer into the metal can be related to the power P of the laser, the radius "a" of the keyhole, the translational speed U of the workpiece and the physical constants of the metal.

The Péclet number P_e is a characteristic of heat transfer in a flowing medium and defines the ratio of convected to conducted heat. It is defined by

$$P_e = \frac{\rho v \ell C_p}{k}$$

where ρ is the density, v is the velocity, ℓ is a characteristic length, k is the thermal conductivity and C_p is the specific heat. The ratio of the viscosity to the thermal conductivity is described by the Prandtl number,

$$P_r = \frac{\mu C_p}{k}$$

and μ is the viscosity. This number is

**Many of the considerations to be discussed in this article are common to electron beam welding, but the mechanism of energy transfer in this case differs from laser beam welding. Both processes, however, cause the keyhole to behave in effect like a heat pipe. Electron beam welds are also subject to a more ragged surface than their laser counterparts.*

important in convective heat transfer problems in fluids since the viscosity can be regarded as a diffusion coefficient of momentum, while the thermal conductivity deals with the diffusion of heat. The Reynolds number is the ratio of the inertia forces, represented by ρv^2 (twice the kinetic energy per unit volume), to the viscous forces, represented by $\mu v/\ell$, so that

$$R = \frac{v\ell}{\mu}$$

Conditions on the fluid motion are as follows: There can be no tangential component of stress at the surface since the mixture of plasma and gas in the keyhole cannot support one. The normal component of the stress, however, need not be constant, since the axial symmetry of the laser and the mechanics of the keyhole are such that to a first approximation the boundary also must have axial symmetry, stress perturbations associated with the metal flow being too small to have a significant effect.

It will be assumed that the variation in size of the keyhole with distance parallel to the beam is sufficiently small for it to have relatively little influence on the flow around the hole, so that the motion is effectively two-dimensional. In practice, this will not always be the case, but in many instances the radial length-scale of variation of temperature is in fact much less than the length-scale parallel to the laser over which the keyhole changes diameter. It will also be assumed that the amount of mass lost by vaporization is unimportant for this calculation, even though, as mentioned above, it plays an important part in the thermodynamics of the process.

In practice, all the physical constants of the material of the workpiece can be expected to depend on temperature; however, these properties will be treated as constant for the most part, allowing only differences between the solid and liquid states. The variations in density between solid and liquid states, or with temperature in a given state, will not be considered.

There is, however, one exception to the above remarks. The viscosity of a liquid normally depends heavily on temperature, and although not much information on the variation of viscosity of liquid metals with temperature is available, there is no reason to suppose they are radically different in this respect. In particular, one should expect the liquid to be substantially less viscous near its boiling point than near its freezing point, and that consequently its flow is likely to be more strongly concentrated near to the keyhole than would be predicted by a model in which the viscosity is constant.

In a recent paper (Ref. 5), several different models of the fluid region were studied. The first model studied, Model 1, is one in which the viscosity is constant. The second, Model 2, is one in which the viscosity is a linear function of temperature, vanishing at the boiling point, but for which the Reynolds number of the flow as a whole is still low. Models 3 and 4 are an attempt to remove the small Reynolds number condition. Model 3 is one in which the liquid is divided into an outer layer, in which the liquid is viscous and the Reynolds number is small, and an inner layer, which is treated as if the liquid were inviscid. One purpose of this model is to demonstrate the way in which the reduction of viscosity with temperature concentrates the flow near the keyhole. It has a second purpose, however, if the Prandtl number is taken to be small (for iron it is 0.057). In this case, it might sometimes be plausible to use an inviscid model for the liquid. The continuity conditions at the interface between the solid and liquid phases are not then entirely obvious, and so Model 3 can be used to investigate what happens when a single inviscid layer is obtained, by taking the limit of Model 3 as the thickness of the viscous layer tends to zero. This limit is Model 4, which describes the liquid motion as that of an entirely inviscid fluid.

The full numerical treatment to solve the partial differential equations related to the laser beam welding problem has also been considered (Ref. 6). The same boundary conditions are used as outlined earlier and only the steady state solution is sought, *i.e.*, the time derivatives are set equal to zero, but all the non-linearities of the Navier Stokes equation are taken into account. All the physical constants associated with laser beam welding are taken as constant with respect to variations in temperature. This is due to a lack of information on the way in which the physical constants of metals vary with temperature, particularly at high temperatures. A Newton-type iteration technique is used to handle the moving boundary at the liquid/solid interface. The initial value of the boundary is generated by the analytical solution to the heat conduction equation for a moving hot circular disk set at the vaporization temperature of the material, thus finding the position of the melting temperature isotherm. The resulting set of partial differential equations are solved by using a technique known as the method of lines. This method is based on converting the partial differential equations into a set of ordinary differential equations by a discretization method. As the partial differential equations are elliptic, artificial time derivatives are added to the ordinary differential equations and one of the fast initial value ordinary differential equation solvers, *e.g.*, the Gear integrator (Ref. 7), is used to integrate the artificial time derivatives to zero, thus obtaining the steady-state solution.

The complete set of equations and boundary conditions that will be considered are as follows:

Solid region

$$U\frac{\partial T}{\partial x} = K_s\nabla^2 T$$

Liquid region

$$\frac{\partial y}{\partial y}\frac{\partial T}{\partial x} - \frac{\partial \psi}{\partial x}\frac{\partial T}{\partial y} = K\nabla^2 T$$

$$\nabla^4\psi = 0$$

where ψ is the stream function satisfying

$$\frac{\partial \psi}{\partial y} = u, \frac{\partial \psi}{\partial x} = -v$$

The quantities u and v are, respectively, the x and y components of the velocity of the molten material.

At r = a, the keyhole radius,

$$\psi = 0$$

$$T = T_v$$

where T_V is the vaporization temperature, and

$$e_{r\theta} = 0$$

i.e., the tangential component of the surface stress vanishes.

This can be rewritten as

$$\frac{\partial \psi}{\partial r} = r\frac{\partial^2 \psi}{\partial r^2}$$

where

$$\frac{\partial \psi}{\partial \theta} = \frac{\partial^2 \psi}{\partial \theta^2} = \ldots = \frac{\partial^n \psi}{\partial \theta^n} = 0.$$

At r = b, the mean position of the interface between the solid and liquid region,

$$\psi = U\, r \sin\theta$$

$$\frac{\partial \psi}{\partial r} = U \sin\theta$$

$$T = T_m$$

where T_m is the melting temperature, and

$$\left[k\nabla T\right]_{\text{Liquid}}^{\text{Solid}} \cdot \nabla S + L\left[\rho\frac{DS}{Dt}\right]_{\text{Liquid}} = 0$$

where L is the latent heat of fusion of the metal. The equation of the boundary is given by

$$S(r,\theta) = 0$$

Lastly, in the solid region

$$T \rightarrow T_o \text{ as } r \rightarrow \infty$$

where T_o is the temperature of the metal

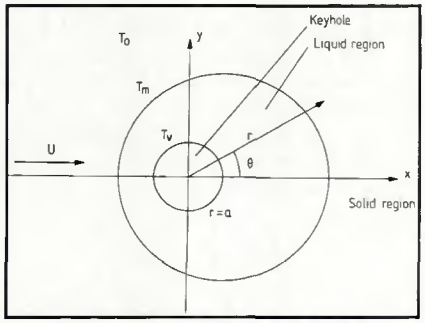

Fig. 3 – Cross-section of the keyhole and molten region for the analytical model showing the two interfaces

far away from the keyhole. There is also the condition that ψ is an odd function of Θ, and T an even function.

The boundary condition between the solid and liquid metal interface can be rewritten as

$$k_s\left[\left(\frac{\partial T_s}{\partial y}\right)+\left(\frac{\partial T_s}{\partial x}\right)\right]^2 - k\left[\left(\frac{\partial T_s}{\partial y}\right)\left(\frac{\partial T_L}{\partial y}\right) + \left(\frac{\partial T_s}{\partial x}\right)\left(\frac{\partial T_L}{\partial x}\right)\right] + \rho L U\frac{\partial T_s}{\partial x} = 0$$

where the subscripts S and L against the variables indicate whether the variables are those of the solid or liquid region.

As the analysis of the various models shows very similar conclusions, attention is restricted here to Model 1. Solutions have been obtained in which the boundaries between the various regions are almost circular and which are consistent with the Oseen type solution for the temperature (Ref. 8). The general configuration is shown in Fig. 3. To construct an analytical solution, it is convenient to use polar coordinates (r,Θ) where

$x = r\cos\Theta$ and $y = r\sin\Theta$

The form of the boundary between the solid and the liquid states is given by

$$S = r - b - U\cos\Theta = 0 \qquad (1)$$

the stream function in the liquid region is

$$\psi = Uf(r)\sin\Theta \qquad (2)$$

and the temperature in the liquid region is

$$T = g(r) + Uh(r)\cos\Theta \qquad (3)$$

In these expressions λ is a constant and f(r) and h(r) are functions of r. The determination of these quantities is part of the solution of the problem. The temperature in the solid region is

$$T \sim T_o + (T_o - T_m)\exp\left(\frac{Ux}{2K_s}\right) \times Ko\left(\frac{Ur}{2K_s}\right) \Big/ \left\{\gamma + \ln\left(\frac{Ub}{4K_s}\right)\right\}$$

[Carslaw and Jaeger (Ref. 9), where T_o is the temperature of the metal far away from the keyhole, K_o is a modified Bessel function and where γ is the Euler-Masheroni constant (γ = 0.57721566).] In Equation 1, the quantity b, the mean radius of the liquid/solid interface, is given by

$$b = \frac{4K_s}{U}\exp\left\{\left(k_s(T_m - T_o)\ln\left(\frac{aU}{4K_s}\right) - \gamma k(T_v - T_m)\right) \Big/ \left(ks(T_m - T_o) + k(T_v - T_m)\right)\right\} \qquad (4)$$

The weld width is in fact 2b.

In Equation 2, the function f(r) is

$$f(r) = [\alpha_1 f_1(r) + \alpha_2 f_2(r)]r$$

where

$$\alpha_1 = \frac{f_2'(b)}{f_1(b)f_2'(b) - f_2(b)f_1'(b)}$$

$$\alpha_2 = \frac{-f_1'(b)}{f_1(b)f_2'(b) - f_2(b)f_1'(b)}$$

$$f_1(r) = \frac{a^2}{r^2} - \frac{r^2}{a^2},\quad f_2(r) = \ln\left(\frac{r}{a}\right)$$

and primes are used to indicate differentiation. Finally, in Equation 3 the functions g(r) and h(r) are given by

$$g(r) = \frac{T_m\ln\left(\frac{r}{a}\right) - T_v\ln\left(\frac{r}{a}\right)}{\ln\left(\frac{b}{a}\right)}$$

and

$$h(r) = \frac{r(T_m - T_v)}{K\ln\left(\frac{b}{a}\right)}$$

$$\left[\left(\frac{K\lambda}{b^2 - a^2} + \alpha_o\right) \times \left(\frac{a^2}{r^2} - 1\right) + \alpha_1 h_1(r) + \alpha_2 h_2(r)\right]$$

where

$$\alpha_o = \frac{\alpha_1 h_1(b) + \alpha_2 h_2(b)}{1 - a^2/b^2}$$

and

$$\lambda = \left[\rho L + \frac{k_s(T_m - T_o)}{K_s(\gamma + \ln(Ub/4K_s))} \times \left(\frac{1}{2} + \gamma + \ln\frac{Ub}{4K_s}\right)\right]\frac{(b^2 - a^2)\ln(b/a)}{2K(T_v - T_m)} + \frac{b(b^2 - a^2)}{2K} \times \left[\alpha_1 h_1'(b) + \alpha_2 h_2'(b) - \frac{2a^2\alpha_o}{b^3}\right]$$

$$h_1(r) = \frac{1}{2}\frac{a^2}{r^2}\ln\left(\frac{r}{a}\right) - \frac{1}{8}\left(\frac{r^2}{a^2} - 1\right)$$

and

$$h_2(r) = \frac{1}{4}\left[\ln\left(\frac{r}{a}\right)\right]^2 - \frac{1}{4}\ln\left(\frac{r}{a}\right)$$

A great amount of concern in laser beam welding is the power required for the process. From the above model, the absorbed power per unit depth can be calculated from the following relation:

$$-\int_{\Theta=0}^{2\pi} a\,k\left.\frac{\partial T}{\partial r}\right|_{r=a} d\Theta$$

where T is the temperature in the molten metal.

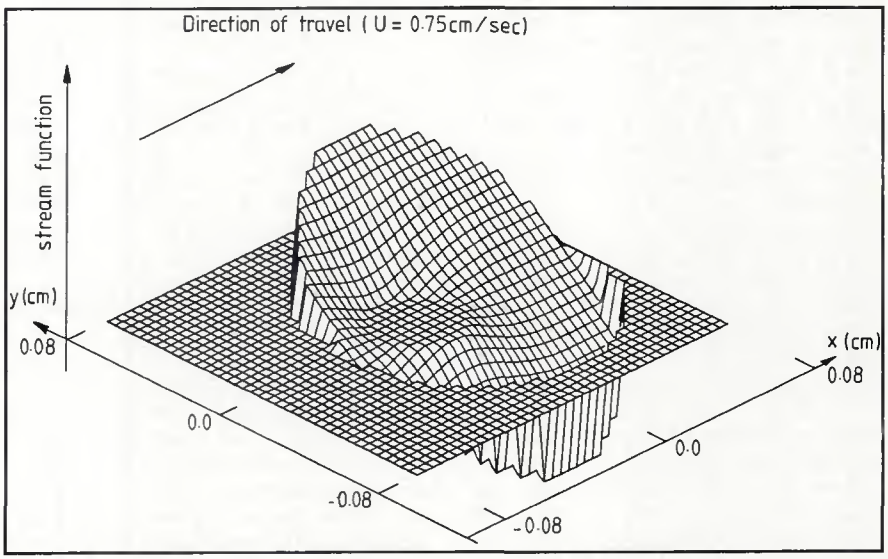

Fig. 4 – The stream function, as a function of (x,y), which ranges from −0.0468 to 0.0468 cm²/s. Note that it is an odd function of y, and for clarity it has been given a value of zero outside the liquid region. The arrow shows the direction of travel of the workpiece

Using the linear approximation given above, one obtains the following expression for the absorbed power per unit depth

$$\frac{-2\pi\,[\,k_s(T_m - T_o) + k(T_v - T_m)\,]}{\gamma + \ln\left(\dfrac{aU}{4K_s}\right)} \qquad (5)$$

This expression does not include the quantity of heat required to vaporize the material and also neglects heat lost by reflection or radiation from the ends of the keyhole, as well as heat convected away in the form of hot gas.

Discussion

Some of the results obtained analytically for the case of Model 1 are displayed in this section. Figure 4 illustrates the stream function, describing the two-dimensional flow of the molten metal around the keyhole as a function of the coordinates (x,y) for a given weld speed U = 0.75 cm/s. For clarity, it is assigned the value zero outside the liquid region. The corresponding contour map of the stream function is illustrated in Fig. 5, where the inner circle denotes the keyhole and the outer curve the interface between the solid and liquid phases. The associated temperature T in the liquid region is shown in Fig. 6. It takes the value T_v inside the keyhole and T_m in the solid region. Figure 7 displays the contour map of the temperature in the liquid region. Figures 8 and 9 give the temperature in the solid region and the corresponding contour map of the temperature.

Using the analytical Model 1, one can study the variation of the keyhole radius "a" with the absorbed laser power P for different values of the weld speed U. The results are displayed in Fig. 10. On the one hand, given the absorbed laser power P together with the assumption of complete absorption of the power, one can predict the diameter of the keyhole, 2a, and the weld width, 2b. To do this, use can be made of Equation 5, which when rearranged gives

$$a = \frac{4k_s}{U}\exp\left\{-2\pi(k_s(T_m - T_o) - k(T_s - T_m)) \Big/ P - \gamma\right\} \qquad (6)$$

A knowledge of the material variables, as well as the absorbed power P when substituted into Equation 6, will give the corresponding value of "a" for the keyhole. Knowing the weld speed U, we can then use Equation 4 to find b and hence the weld width 2b. The variation of the weld width 2b against the laser power P for different weld speeds U is displayed in Fig. 11.

Alternatively, one can calculate the least value of the power P needed to produce a weld, and predict the weld width for a given translational speed U of the workpiece and a given size, a, of the keyhole. If the material variables of the workpiece are known, together with the values of U and a, then Equation 5 can be used to evaluate the power per unit depth. Using the same parameters together with Equation 4 for b then gives the value of the weld width 2b.

Turning next to the shape of the molten region, Fig. 12 shows it for a weld speed U = 0.75 cm/s, with the cross-section of the keyhole and the position of the analytically evaluated moving boundary at the solid/liquid interface. Curve (a)

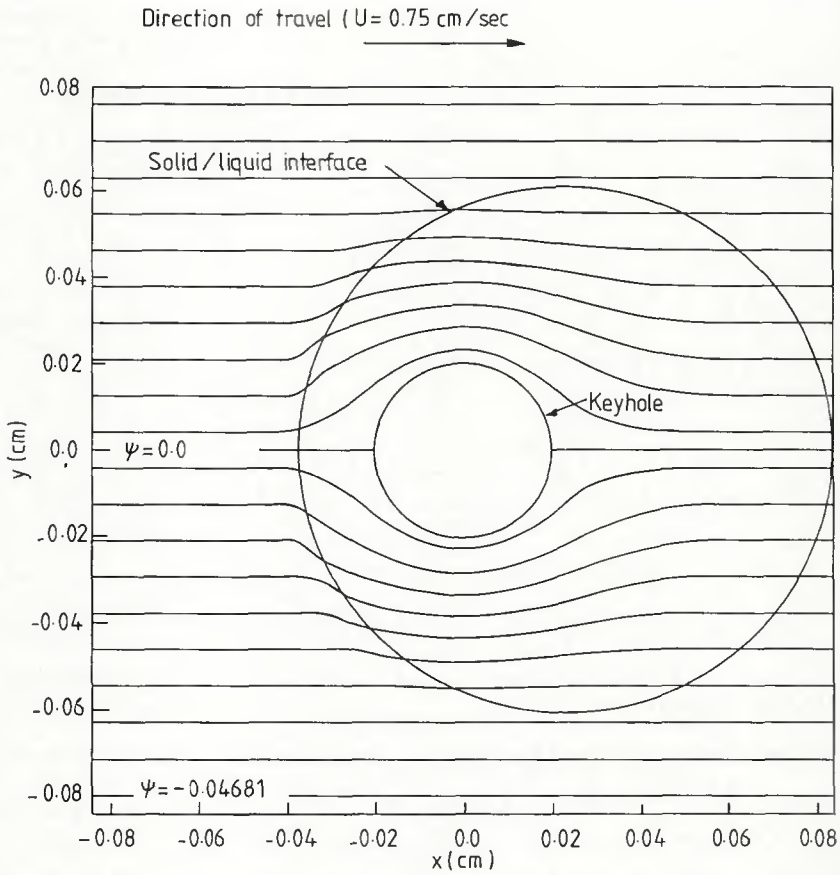

Fig. 5 — The contour map of the stream function. The contours are at multiples of 0.00629 cm²/s

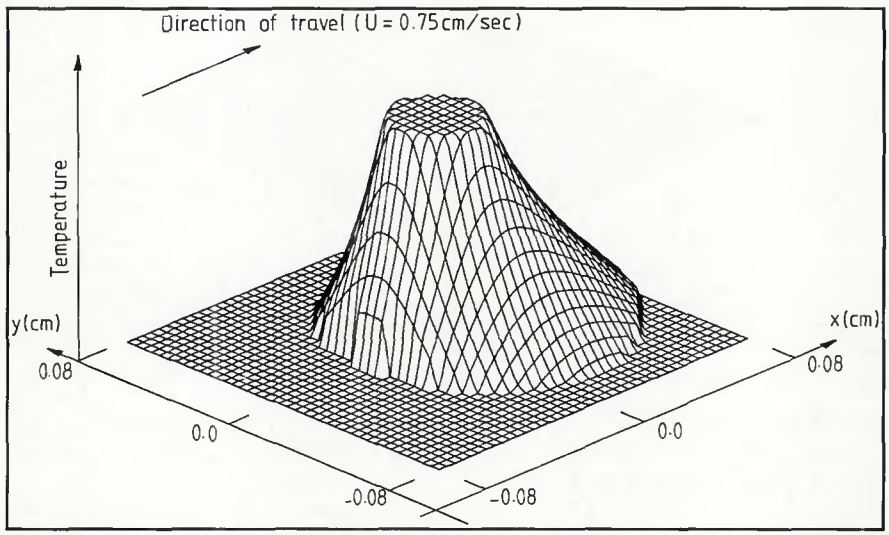

Fig. 6 — The temperature in the liquid region, which ranges from 1371.1°C to 2726.8°C. For clarity, T has been given the value of T_v inside the keyhole and T_m in the solid region. Direction of travel of the workpiece is indicated by an arrow

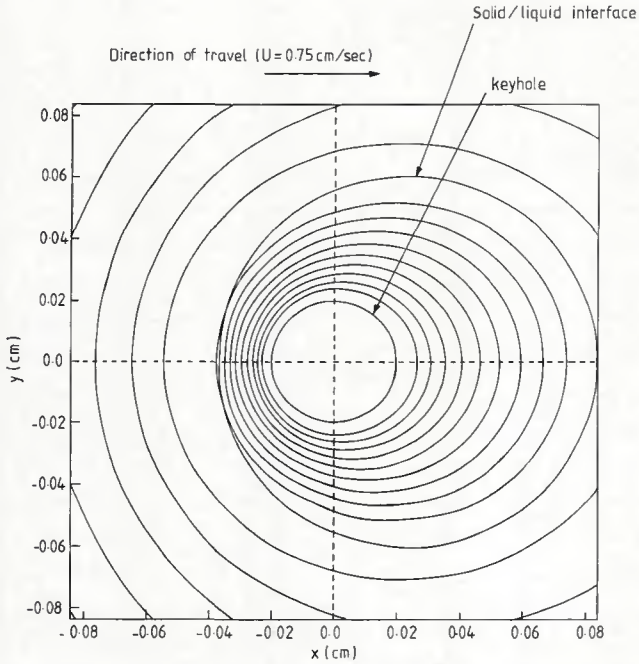

Fig. 7 — The contour map of the temperature in the liquid region. The contours are at multiples of 109.07°C

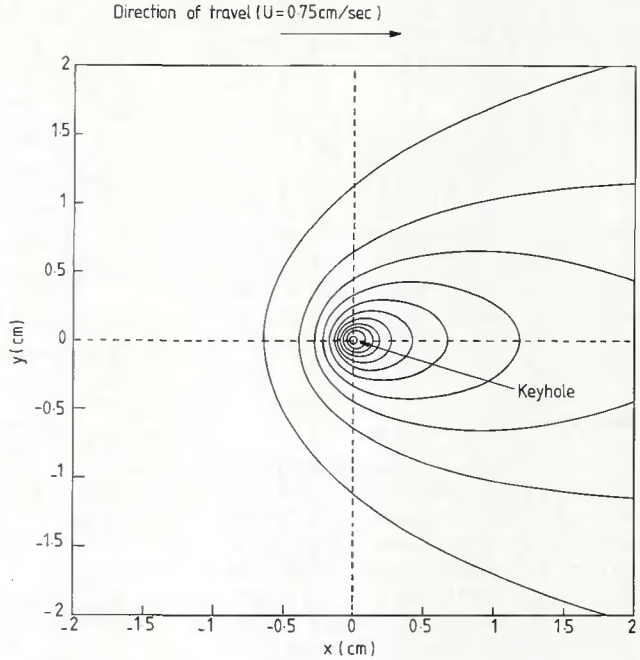

Fig. 9 — The contour map of the temperature in the solid region. The contours are at multiples of 135.1°C

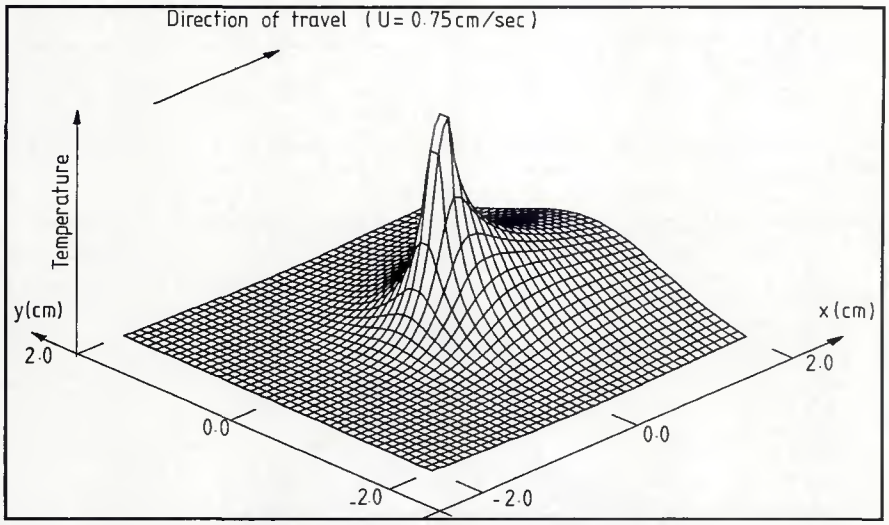

Fig. 8 — The temperature in the solid region ranges from 20.064° to 1371.1°C. For clarity, T has been given the value of T_m inside the liquid region

in the figure is included to illustrate the shape of the moving boundary as calculated by the full numerical model (Ref. 6). Figure 12 clearly shows the very close agreement between the analytical and numerical treatments. The largest difference is evident at the rear of the molten region.

If one compares the shape of the molten region as evaluated above with a horizontal cross-section of an actual weld some depth below the surface, one can be confident that the neglect of surface tension effects in the treatment given here will be valid. If one moves to the actual surface of a weld, one would expect a small variation to arise in the shape of the moving boundary to the rear of the molten region, due to surface tension effects.

The position of this boundary may, however, in an extreme case involving high weld speeds, be ill-defined near the tail end of the weld pool when the material is an alloy. This could arise because different phases of the same material might coexist in thermodynamic equilibrium, leading to a mushy region. Andrews, Atthey and Byatt-Smith (Ref. 10) indicate that the length scale of this could be of order 10^{-5} m. Hence, in most cases, this effect could probably be ignored.

Turning next to the variation of the position of the moving boundary at the solid/liquid interface with weld speed, Fig. 13 illustrates it for four different weld speeds, the inner circle denoting the position of the keyhole.

To study the variations in the laser beam welding process when different materials are employed, a graph is included of the numerically and analytically evaluated absorbed laser power against various weld speeds, using a fixed keyhole of radius 0.01 cm in every case — Fig. 14. The typical materials chosen are titanium, iron, aluminum and lead because their material variables cover the widest range, although lead itself is not normally considered to be a welding material.

The models of laser beam welding presented here agree with the experimental welding process in all its general features. In the absence of any known comprehensive quotations of all the relevant variables involved in the problem in connection with the experiment, agreement is necessarily restricted to a qualitative level, as, in fact, is agreement with the work of other investigators, such as Mazumder and Steen (Ref. 2).

Figure 15 shows a cross-section of a completed demonstration weld. It will be noticed that there is a substantial weld bead on the upper surface, and a much smaller but, nonetheless, prominent one on the lower surface as well. Associated with both, but especially the upper one, is a region that corresponds to a basin shape for the weld pool, and these are joined by a thinner, somewhat wedge-shaped region. It is predominantly this part of the weld to which the work described here applies. The flow in this

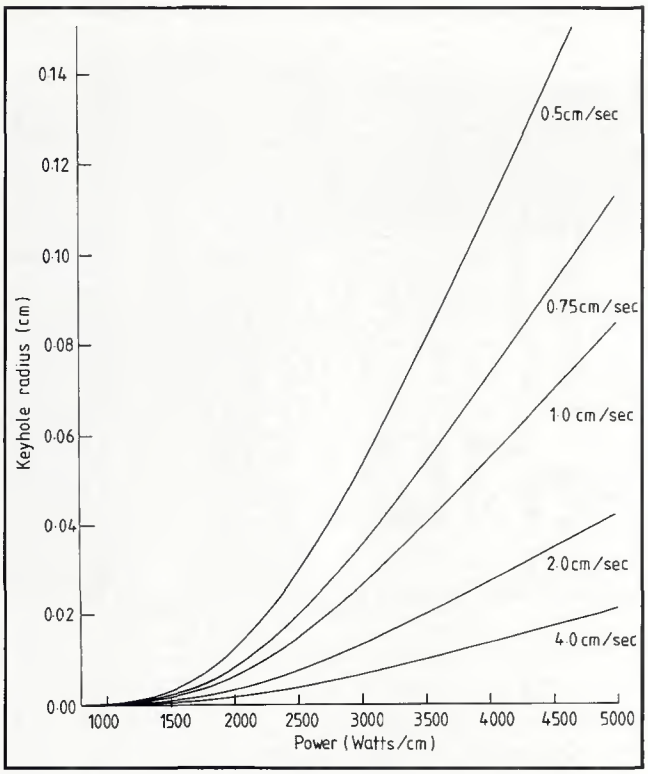

Fig. 10 — The graph of the keyhole radius against the absorbed power for different weld speeds for iron

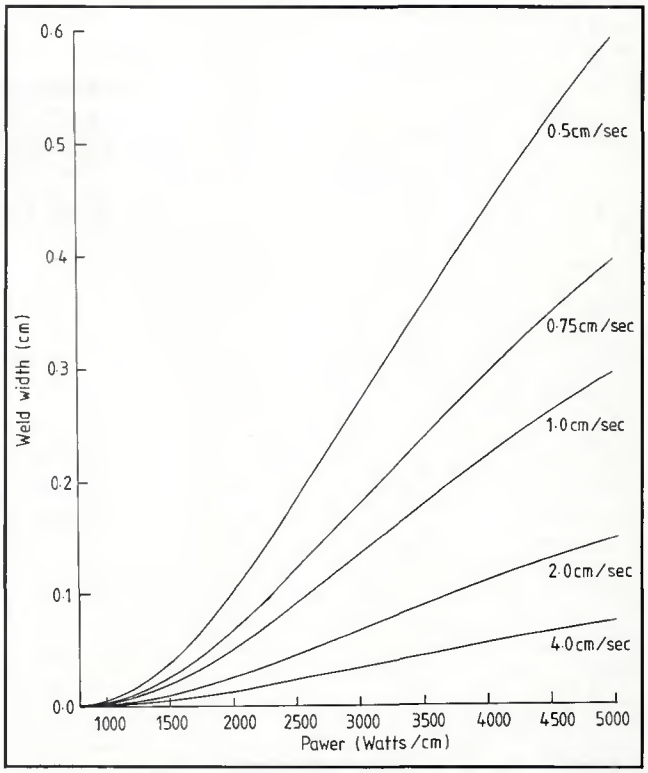

Fig. 11 — The graph of the weld width against the absorbed power for different weld speeds for iron

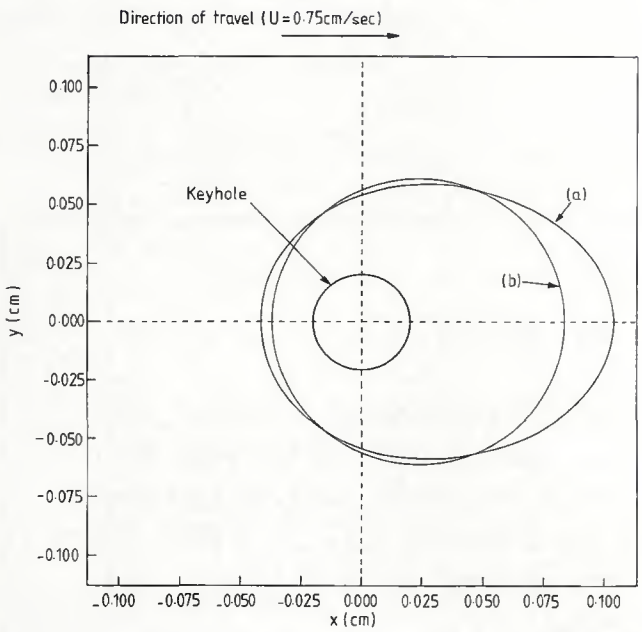

Fig. 12 — Cross-section of the keyhole and the molten region, showing the position of the moving boundary at the solid/liquid interface. Curve (a) corresponds to the moving boundary, as calculated by the numerical model, and curve (b) corresponds to the analytical moving boundary

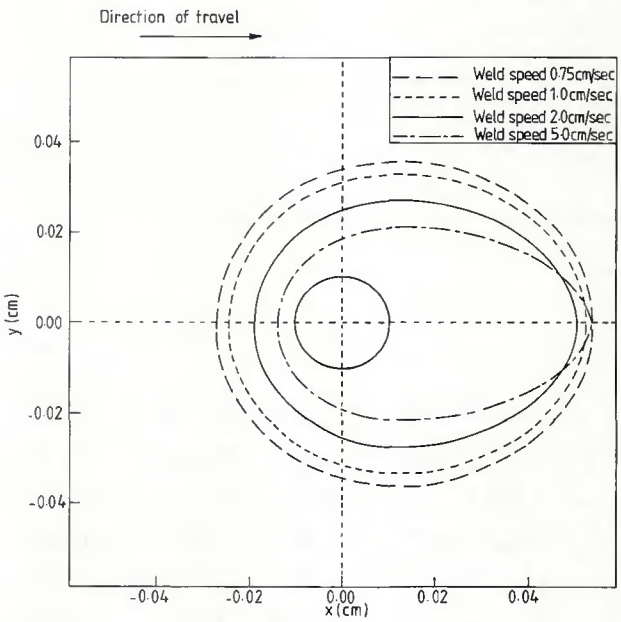

Fig. 13 — The cross-section of the keyhole and molten region for iron, showing the position of the moving boundary at the solid/liquid interface for four different speeds, using the numerical model

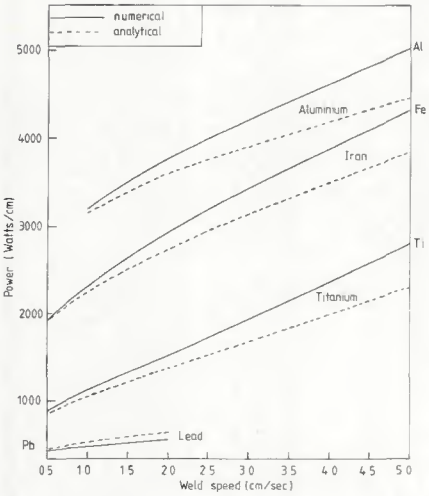

Fig. 14 — The graph of the numerical and analytical absorbed power plotted against the weld speed for aluminum, iron, lead and titanium. (Keyhole radius = 0.01 cm)

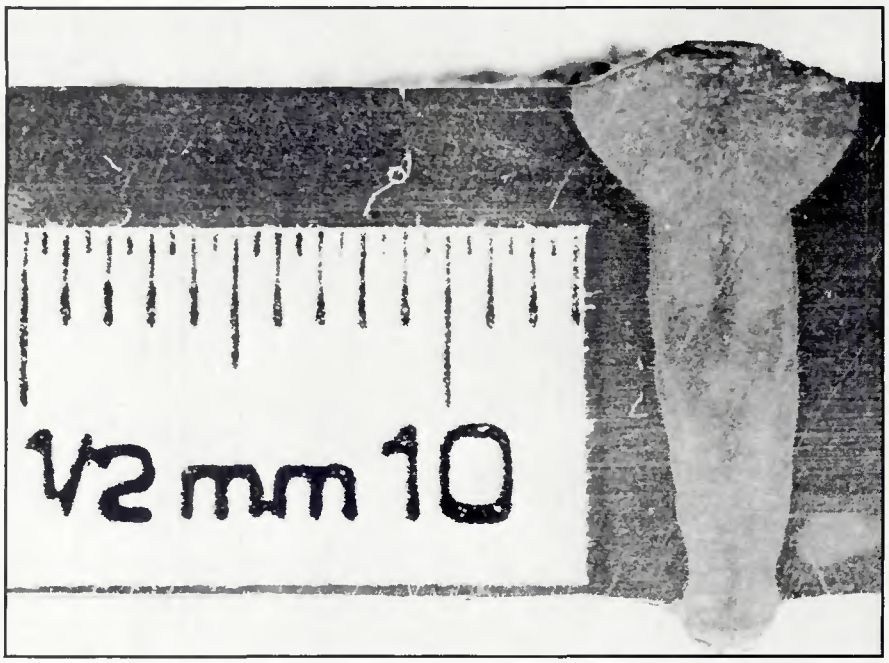

Fig. 15 — Cross-section of the complete weld showing the upwelling on both sides of the weld

region can be expected to be more nearly two-dimensional than in the regions near the two ends. The experiments of Arata, *et al.* (Ref. 11), using x-rays and glass have shown that there is motion in the third dimension of the weld. This will be most noticeable in the large weld pool at the surface. In the narrow region it will be less noticeable and can be represented by a mean flow with only a small overall drift parallel to the axis. It is this mean flow which is represented here, and the motion parallel to the axis is ignored.

Conclusion

From the information above, it is clear that the analytical model described here is appropriate to fairly small values of the Péclet number. Extension to intermediate values can be done numerically, and the flow obtained. The calculated power absorbed applies to the central part of the keyhole and the surrounding molten region. The results obtained here can be used to calculate the total power absorbed in this region, if there is knowledge of the way in which the keyhole radius, a, varies with depth in the workpiece. This dependence is not simple to predict, as it will depend on a number of factors. Internal reflection in the keyhole and the setting of the laser optics are examples of an internal and an external mechanism that have a bearing on it, and which inevitably contribute to the final weld shape.

References

1. Andrews, J. G. 1979. *Bull. Inst. Maths. Applics.* 15:250–253.
2. Mazumder, J., and Steen, W. M. 1980. *J. Appl. Phys.* 51:941–947.
3. Swift-Hook, D. T. and Gick, A. E. F. 1973. Penetration welding with lasers. *Welding Journal* 52(11):492-s to 499-s.
4. Andrews, J. G., and Atthey, D. R. 1976. *J. Phys. D: Appl. Phys.* 9:2181–2194.
5. Dowden, J. M., Davis, M., and Kapadia, P. 1983. *J. Fluid Mech.* 126:123–146.
6. Davis, M., Kapadia, P., and Dowden, J. M. 1985. *J. Comp. Phys.* 60:534–548.
7. Hindmarsh, A. C. 1973. UCRL-30059, Lawrence Livermore Laboratory report.
8. Lamb, H. 1932. *Hydrodynamics.* Cambridge.
9. Carslaw, H. C., and Jaeger, J. C. 1959. *Conduction of Heat in Solids.* Clarendon Press, Oxford.
10. Andrews, J. G., Atthey, D. R., and Byatt-Smith, J. G. 1980. *J. Fluid Mech.* 100:785–800.
11. Arata, Y., Maruo, H., Miyamoto, I., and Inoue, Y. 1977. IIW DOC IV/222/77.

Reminder to Authors

Please note that completed Author Application Forms and accompanying 500-word summaries must be mailed by July 15, 1986, to ensure consideration for the Professional Program of the 68th Annual AWS Convention, to be held March 22–27, 1987, in Chicago, Ill. Author Application Forms appear on p. 112-s in the April 1986 issue of the *Welding Journal*.